Luminescence Properties and Electronic Structure of Some Quinolizinone and Indolizinone Derivatives

Sn. Bakalova [1], P. Nikolov [1], E. Stanoeva [2], V. Ognyanov [1], and M. Haimova [2]

[1] Institute of Organic Chemistry with Centre of Phytochemistry, Bulgarian Academy of Sciences, 1040 Sofia, Bulgaria
[2] Faculty of Chemistry, University of Sofia, 1126 Sofia, Bulgaria

Z. Naturforsch. **47a**, 521–526 (1992); received October 29, 1991

The absorption and luminescence static and dynamic properties of a group of quinolizinone and indolizinone derivatives in solvents of different polarity at 297 K and 77 K are studied. On the basis of the spectral data and the PPP quantum-chemical results the problem of the main chromophore in these structures is discussed.

Key words: Absorption, Luminescence, Quinolizinones, Indolizinones.

1. Introduction

In this paper the absorption and luminescence properties of some heterocycles incorporating the quinolizine [1] or indolizine [2] ring system are studied. The investigated compounds **1** [3], **2a–b** [4], **3** [4], **4a–b** [5], **5** [5] and **6a–c** [6] are shown in Figure 1. There are no data in the literature on their luminescence properties. Quantum chemical investigations have been performed to elucidate which is the main chromophore.

2. Spectral Properties

a) Absorption Characteristics

The absorption spectra are recorded on a double beam spectrophotometer Specord M 40 (Carl Zeiss, Jena), and the luminescence spectra on a Perkin Elmer MPF-44 spectrofluorimeter. The solvents used are of spectroscopic grade. The fluorescence quantum yields are determined relative to 3-aminophthalimide ($Q_F = 0.6$ in ethanol [7]). The fluorescence lifetimes are measured on a nanosecond spectrofluorimeter PRA 2000 at room temperature. The low-temperature luminescence measurements are performed at 77 K in the standard phosphorescence accessory to MPF-44 in quartz tubes of 4 mm diameter.

Reprint requests to Dr. P. Nikolov, Institute of Organic Chemistry with Centre of Phytochemistry, Bulgarian Academy of Sciences, Akad. G. Bontchev, bl. 9, 1040 Sofia, Bulgaria.

The compounds shown in Fig. 1 can be divided into two main groups A and B. Group A consists of the compounds **1**, **2a–b**, and **4a–b**, which may be regarded as derivatives of the parent 8 H-benzo[a]-

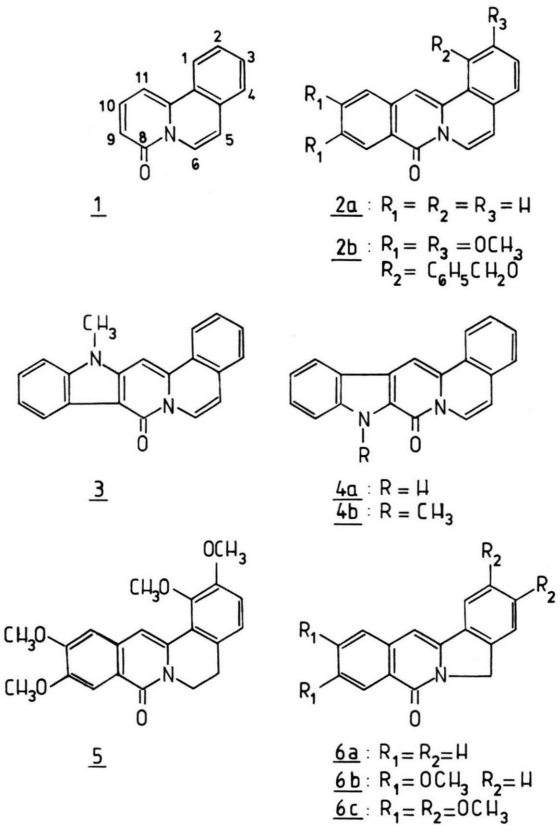

Fig. 1. Structure of the compounds investigated.

0932-0784 / 92 / 0300-0521 $ 01.30/0. – Please order a reprint rather than making your own copy.

Table 1 a. Experimental spectra characteristics of the investigated compounds in ethanol. ν_{abs} and ν_{fl}: energy of the longest wavelength absorption and the fluorescence Franck-Condon transition in cm^{-1}; ε: molar absorptivity in 10^3 l mol^{-1} cm^{-1}; Q_F: fluorescence quantum yield.

	ν_{abs}	ε	ν_{fl}	Q_F
1	25 700, 24 200	13.8, 12.0	23 470, *22 470*	0.28
2a	26 500, 25 200, 23 800	16.1, 17.1, 12.6	23 500, *22 200*, 21 000	0.22
2b	27 200, 25 500, 24 150	10.7, 15.6, 14.7	23 700, *22 500*, 21 200	0.25
3	26 900, 25 600, 24 200	9.8, 16.1, 15.8	23 420, *22 170*, 20 830	0.52
4a	26 200, 24 800, 23 500	11.7, 13.2, 11.6	23 000, *21 830*, 20 500	0.34
4b	25 600, 24 200, 22 900	14.7, 18.2, 17.4	22 520, *21 370*, 20 000	0.41
5	30 500, 28 900, 27 600	19.0, 17.0, 13.1	25 300	0.26
6a	30 900, 29 500, 28 050	10.3, 7.9, 5.3	27 200, *26 100*, 25 100	0.32
6b	30 800, 29 620, 28 100	26.2, 27.2, 19.6	27 400, *26 100*, 24 900	0.47
6c	30 200, 29 150, 27 650	25.5, 24.7, 14.5	25 100	0.26

Table 1 b. Experimental spectral characteristics of the investigated compounds in acetonitrile and cyclohexane.

	Solvent	ν_{abs}	ν_{fl}	Q_F
2a	Acetonitrile	26 500, *25 200*, 23 800	23 420, *22 220*, 21 000	0.23
	Cyclohexane	26 300, *25 100*, 23 650	23 530, *22 270*, 21 050	0.24
2b	Acetonitrile	26 700, *25 400*, 24 000	23 640, *22 420*, 21 140	0.36
	Cyclohexane	26 800, *25 200*, 23 800	23 530, *23 200*, 21 000	0.38
5	Acetonitrile	30 200, *28 900*, 27 600	26 670, *25 380*, 24 100	0.23
6a	Acetonitrile	30 800, *29 500*, 28 050	27 250, *25 970*, 24 750	0.33
	Cyclohexane	30 500, *29 300*, 27 900	27 550, *26 100*, 24 800	0.42
6b	Acetonitrile	30 500, *29 420*, 27 950	27 250, *25 970*, 24 690	0.62
	Cyclohexane	30 500, *29 050*, 27 500	27 250, *25 740*, 24 240	0.66
6c	Acetonitrile	30 200, *29 100*, 27 700	27 030, *25 700*, 24 330	0.27
	Cyclohexane	30 200, 29 000, 27 450	27 250, *25 770*, 24 330	0.33

quinolizin-8-one (compound **1**) in which a new aromatic system is condensed along the *g* bond. The members of group B (**5** and **6a–c**) may be regarded as substituted isoquinolinones with a fixed planar structure; they are analogs of the compounds in group A, in which the Ch=CH group in position 5–6 is substituted for a CH_2–CH_2 or a CH_2 one.

Table 1 shows some basic spectral characteristics of the compounds.

The longest wavelength absorption band is around 24 000 cm^{-1} in the compounds of group A, while that of the compounds in group B is shifted towards shorter wavelengths and is around 28 000 cm^{-1}. In all compounds, at shorter wavelengths there is a series of absorption transitions of higher intensity.

Figure 2 (above) shows the absorption and fluorescence spectrum of the parent compound of group A **1** in ethanol, as well as the computed transition energies and oscillator strengths in the PPP–SCF–CI approximation (denoted by vertical lines). The absorption spectra of **2a–b** and **3** are similar in shape and position to that of **1**. However, in the absorption spectra of compounds **4a–b** a new long wavelength maximum is observed around 23 000 cm^{-1}, which according to PPP quantum-chemical calculations (see Tables 1 and 4) is localized on the indole fragment.

Figure 2 (below) shows the absorption and fluorescence spectrum of compound **6a**, a typical representative of group B, as well as the computed transition energies and oscillator strengths. The electronic spectra of the other compounds in this group are very similar to those of **6a** (see Table 1).

The position of the longest wavelength absorption maximum of the compounds is almost independent of the solvent polarity; a slight hypochromic shift (not more than 500 cm^{-1}) is observed on changing the solvent from ethanol and acetonitrile to cyclohexane.

The $n\pi^*$ transitions of the compounds cannot be observed in the absorption spectra, as they are overlapped by the intense $\pi\pi^*$ transitions. Having in mind that the position of the $n\pi^*$ transition localized on the carbonyl group is practically independent of the length of the conjugated π-electronic system [8, 9], the energy of the lowest singlet $n\pi^*$ transition may be

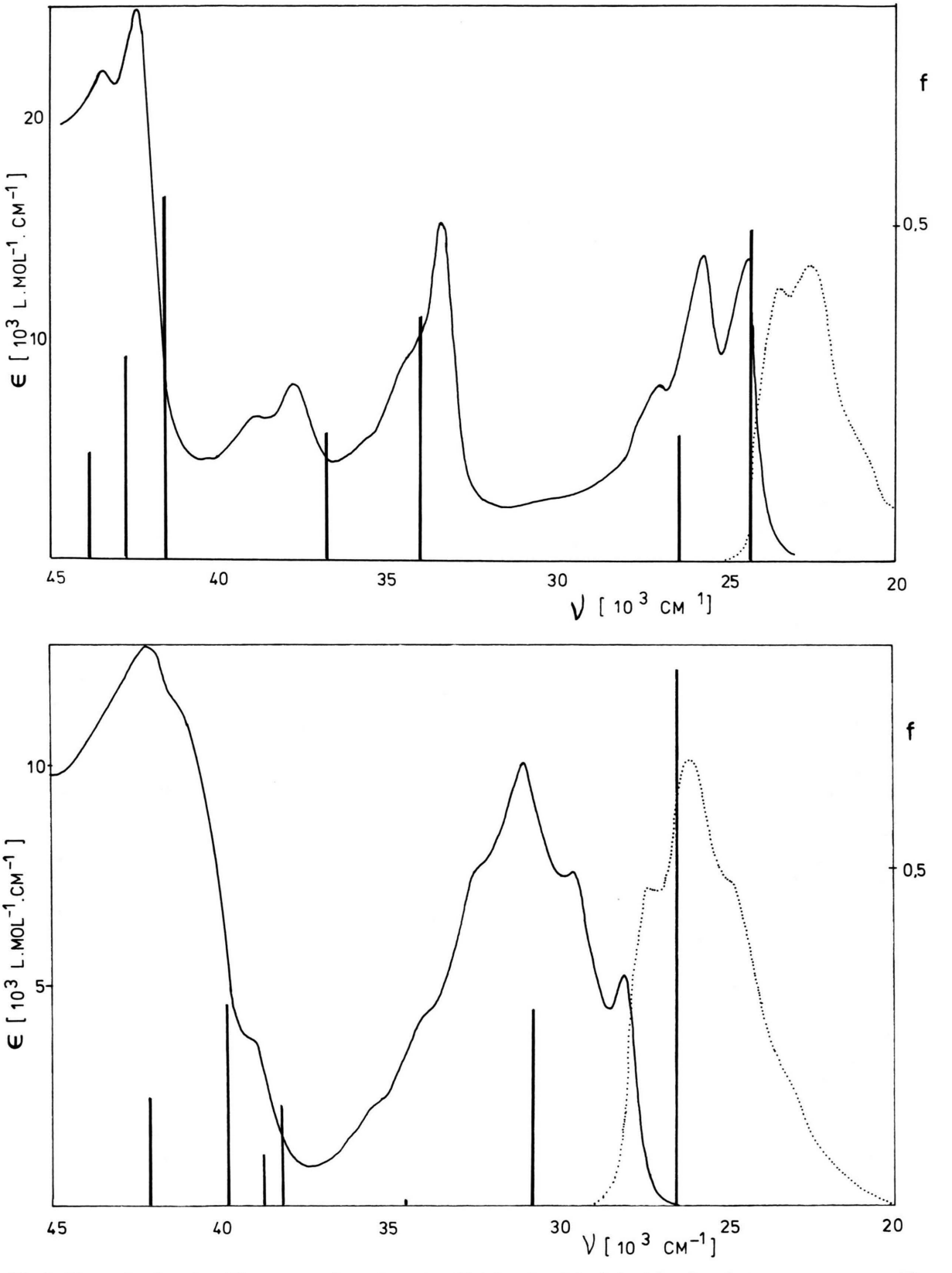

Fig. 2. Absorption (——) and fluorescence (· · · · ·) spectra of **1** (above) and **6a** (below) in ethanol at room temperature. The vertical lines denote the computed energy of the singlet $\pi\pi^*$ transitions and the corresponding oscillator strengths f.

evaluated by analogy with aromatic ketones with similar structure, for example the unsubstituted coumarin in which $\nu_{n\pi^*} > 32\,000\ cm^{-1}$ [10]. The high fluorescence quantum yields of the compounds indicate that the energy of the O–O transition of the lowest singlet $n\pi^*$ state is really considerably higher than that of the $S_1(\pi\pi^*)$ state, which, according to the experimental and theoretical data, has an energy not exceeding 28 000 cm^{-1}.

b) Luminescence Characteristics

All of the studied compounds fluorescence in solution at room temperature in the region 27 000–20 000 cm^{-1} (Table 1). The fluorescence spectra of most of them possess a well defined vibrational structure. The fluorescence spectra of **2a–b** and **3** are similar in position to that of **1**, while those of compounds **4a–b** are shifted to the red. The fluorescence and absorption spectra of the compounds in group B are shifted to shorter wavelengths in comparison to those in group A.

The Stokes shift, evaluated from the energy difference of the absorption and fluorescence maxima, is 3000–4000 cm^{-1}. The increase of the solvent polarity (cyclohexane, acetonitrile, ethanol) leads to a slight hypochromic shift (not more than 600 cm^{-1}) of the fluorescence Franck-Condon transitions and an insignificant change (up to 1000 cm^{-1}) of the Stokes loss (see Table 1). The change of the dipole moment of the compounds upon excitation evaluated according to the model of Lippert [11] does not exceed 2–3 D.

All of the studied compounds have relatively high fluorescence quantum yields in solution at room temperature. The fluorescence intensity is not substantially influenced by the solvent; the fluorescence quantum yields are somewhat higher in cyclohexane than in acetonitrile and ethanol (see Table 1).

Table 2 shows the lifetime τ of the $S_1(\pi\pi^*)$ state, computed from the fluorescence decay curve, and the radiative and non-radiative rate constants, calculated from τ and Q_F. Both the singlet lifetime and the transition constants are of the same order of magnitude as those of compounds of similar structure – e.g. substituted iso-coumarins [12].

Table 3 shows some luminescence characteristics of the compounds in frozen ethanol solutions at 77 K.

The freezing of the ethanol solutions leads to the well-known [13] blue shift of the Franck-Condon fluorescence transition; in most cases the fluorescence intensity increases slightly (up to 4 times), and a weak phosphorescence emission is observed. The S–T splitting is in the range 4000–7000 cm^{-1}.

Table 2. Natural lifetime τ and rate constants of radiative (k_R) and radiationless (k_{NR}) deactivation of S_1, calculated from τ and Q_F at 293 K in ethanol; τ is calculated from the fluorescence decay curve, fitted to a monoexponential linear function $I(t) = A \exp(-t/\tau)$; χ is the mean error of fitting; $[\tau] = ns$, $[k] = ns^{-1}$.

	τ	χ	k_R	k_{NR}
1	2.11	0.90	0.133	0.341
2a	2.83	1.10	0.077	0.276
3	3.83	1.08	0.136	0.125
4a	3.28	1.02	0.104	0.201
4b	2.50	1.04	0.164	0.236
5	1.80	1.38	0.144	0.411
6a	3.18	0.90	0.101	0.214
6a	3.30	1.27	0.142	0.161

Table 3. Spectral characteristics in frozen ethanolic solutions at 77 K.

	ν_{fl}	$\frac{I^{fl}(77\ K)}{I^{fl}(293\ K)}$	ν_{ph}
2b	24 000, *22 800*, 21 400	3.5	18 700, 17 500
5	25 800, *24 500*, 23 000	3.0	20 000, 18 500
6b	27 900, *26 600*, 25 100,	4.0	19 900, 18 400
6c	*26 000*, 24 600	0.7	20 000, 18 200

Because of the fixed planar structure of the compounds, quenching processes due to intramolecular motion of certain fragments in the molecule should not be significant; this is supported by the relatively high fluorescence quantum yields observed in solution at room temperature, as well as the insignificant increase of the fluorescence intensity in a solid matrix at 77 K.

3. Quantum-chemical Investigations

The quantum-chemical calculations were carried out in π-electron approximation by the PPP–SCF–CI method [14] with a standard parameterization [15]. The absorption spectra agree well with the quantum-chemical calculations, the difference between the calculated and the experimental Franck-Condon transition energies being within the accuracy of the PPP method (0.1–0.2 eV). Fig. 2 allows comparison of the

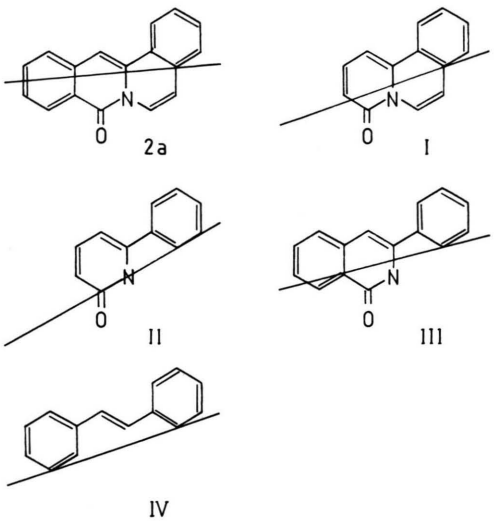

Fig. 3. Direction of the computed transition moment of the longest wavelength $\pi\pi^*$ transition of **2a** and the fragments I–IV.

absorption spectra of **1** and **6a** and the calculated transition energies and oscillator strengths.

The quantum-chemical calculations were used to propose a main chromophore in some of the compounds. The conclusions are made by comparison of the theoretical PPP results, namely the computed transition energies, direction of the transition moments and configuration analysis of the molecule and its fragments. A similar approach for identification of the main chromophore was applied e.g. in [16]. Some of the above criteria were also used in [17].

Figure 3 shows the fragments I–IV, which may be considered on the basis of the principle of structural analogy as main chromophores of compounds **2a** (I–IV), **4a** (I–III) and **6a** (II–IV).

The analysis of the wave functions (Table 4) shows that for **2a** and I the longest wavelength $\pi\pi^*$ transition is determined by the HOMO-LUMO transition (the statistical weight of the $V_1^{1'}$ configuration is >0.90), while the second $\pi\pi^*$ transition is determined predominantly by the $V_1^{2'}$ configuration.

Because of the character of the transitions, the energies and the oscillator strengths of **2a** are similar only to those of I (see Table 4), the latter is the only fragment from the considered ones which may be regarded as the main chromophore of **2a**.

As seen in Fig. 3 there is no significant difference in the direction of the calculated transition moments for **2a** and I, which supports the conclusion in the previous paragraph. However, it should be noted that the direction of the transition moments of the other possible fragments is also very similar.

Table 4. Theoretical values of the energies of the first $\pi\pi^*$ electron transitions ΔE (in eV), oscillator strengths (f) and coefficients of the predominating configurations ($d_{kk'}$) in the CI wave fuctions for compounds **2a**, **4a**, **6a** and the corresponding fragments I, II, III and IV.

	ΔE	f	$d_{kk'}$
2a	3.08	0.609	$0.96\ V_1^{1'}$
	3.19	0.320	$-0.97\ V_1^{2'}$
	3.77	0.091	$0.16\ V_1^{1'} - 0.92\ V_1^{3'}$
4a	2.83	0.258	$0.74\ V_1^{1'} + 0.32\ V_1^{2'} - 0.43\ V_2^{1'}$
	2.94	0.342	$-0.52\ V_1^{1'} + 0.71\ V_1^{2'} - 0.33\ V_2^{1'}$
	3.20	0.133	$0.21\ V_1^{1'} + 0.42\ V_1^{2'} - 0.35\ V_2^{1'} + 0.69\ V_1^{3'}$
6a	3.29	0.798	$0.96\ V_1^{1'}$
	3.81	0.191	$-0.18\ V_1^{1'} + 0.90\ V_1^{2'}$
	4.28	0.002	$0.73\ V_1^{3'} - 0.55\ V_3^{1'}$
I	2.98	0.485	$-0.95\ V_1^{1'} + 0.23\ V_1^{2'}$
	3.28	0.184	$-0.23\ V_1^{1'} - 0.95\ V_1^{2'}$
	4.21	0.368	$0.42\ V_1^{3'} - 0.58\ V_2^{1'} + 0.53\ V_2^{2'}$
II	3.20	0.597	$-0.98\ V_1^{1'}$
	4.34	0.000	$-0.64\ V_1^{2'} - 0.63\ V_2^{1'} - 0.35\ V_3^{2'}$
	4.64	0.168	$0.89\ V_1^{3'} + 0.27\ V_3^{1'} + 0.23\ V_4^{1'}$
III	3.33	0.828	$0.97\ V_1^{1'}$
	3.90	0.141	$0.88\ V_1^{2'} + 0.34\ V_2^{1'}$
	4.33	0.001	$-0.70\ V_1^{3'} - 0.56\ V_3^{1'} - 0.34\ V_4^{3'}$
IV	3.48	1.239	$-0.99\ V_1^{1'}$
	4.14	0.000	$-0.65\ V_1^{2'} - 0.65\ V_2^{1'}$
	4.30	0.000	$0.65\ V_1^{3'} - 0.65\ V_3^{1'} + 0.26\ V_4^{3'} - 0.26\ V_3^{4'}$

Table 5. Luzanov values L_f [17], indicating the degree of localization of the $^1S_0 \rightarrow {}^1S_i$ ($i=1, 2$) transitions for **4a** and for the indole fragment (V) and fragment I. As atoms 9 and 10 are included in both fragments, $\sum L_f > 1$.

Fragment	I	V
$L_f\ (^1S_0 \rightarrow {}^1S_1)$	0.445	0.700
$L_f\ (^1S_0 \rightarrow {}^1S_2)$	0.743	0.352

The results from the PPP calculations of **4a** (see Table 4) indicate that the $S_0-S_1(\pi\pi^*)$ transition of fragment I corresponds to the $S_0-S_2(\pi\pi^*)$ transition of compound **4a**; this conclusion is confirmed by the results of the analysis performed by the Luzanov method [18], see Table 5. The data in Table 5 also show that the $S_0-S_1(\pi\pi^*)$ transition of compound **4a** is localized on the indole fragment.

On the basis of the PPP computations a main chromophore of compound **6a** could not be proposed.

The available experimental data on the electronic spectra of compounds **2a**, **4a**, **6a**, I, III and IV also support the conclusions drawn on the basis of the quantum-chemical results. The spectral characteristics (transition energies, molar absorptivities and fine structure) of the studied quinolizinone (e.g. **2a**, **6a**) and indolizinone (e.g. **4a**) derivatives are quite different from those of stilbene (IV) and isoquinolinone (III), while the electronic spectra of **1** (I) and **2a** are very similar (Table 1).

[1] G. Jones, in: Advances in Heterocyclic Chemistry (A. R. Katritzky, ed.) vol. 31, Academic Press, New York 1982.
[2] F. J. Swinbourne, J. H. Hunt, and G. Klinkert, in: Advances in Heterocyclic Chemistry (A. R. Katritzky, ed.), vol. 23, p. 103, Academic Press, New York 1978.
[3] E. Stanoeva, M. Haimova, and V. Ognyanov, Lieb. Ann. Chem. **1984,** 389.
[4] V. I. Ognyanov, M. A. Haimova, and N. M. Mollov, Heterocycles **19,** 1069 (1982).
[5] E. Stanoeva, M. Haimova, N. Mollova, and S. Popov, God. Sof. Univ. "Kl. Okhridski", Khim. Fak. **79,** 458 (1985) (Publ. 1990); CA **114,** 42602a (1991).
[6] V. I. Ognyanov, M. A. Haimova, and N. M. Mollov, Mh. Chem. **113,** 993 (1982).
[7] N. Borisovitch, V. Zelinskii, and B. Noperent, Dokl. Akad. Nauk USSR **94,** 37 (1954).
[8] A. El-Sayed and W. Robinson, J. Phys. Chem. **34,** 1480 (1961).
[9] J. Fabian and H. Hartmann, Light Absorption of Organic Colorants: Theoretical Treatment and Empirical Rules, Springer-Verlag, Berlin 1980.
[10] T. A. Moore, M. L. Harter, and P. S. Song, J. Mol. Spectrosc. **40,** 144 (1971).
[11] E. Lippert, Z. Electrochem. **61,** 962 (1957).
[12] P. Nikolov, N. Tyutyulkov, and V. Dryanska, Z. Naturforsch. **42a,** 987 (1987).
[13] R. Becker, Theory and Interpretation of Fluorescence and Phosphorescence, Wiley Interscience, New York 1969.
[14] R. G. Parr, Quantum Theory of the Molecular Electronic Structure, Benjamin, New York 1964.
[15] F. Fratev, G. Hibaum, and A. Gochev, J. Mol. Struct. **23,** 437 (1974).
[16] P. Nikolov, T. Deligeorgiev, N. Tyutyulkov, and I. Kanev, Z. Naturforsch. **43a,** 793 (1988).
[17] M. Klessinger, Tetrahedron **22,** 3355 (1966).
[18] A. Luzanov, Uspechi Chimii (USSR) **49,** 2086 (1980).